Field-Driven Quantum Criticality in the Spinel Magnet $ZnCr_2Se_4$

C. C. Gu,[1] Z. Y. Zhao,[2,3] X. L. Chen,[1] M. Lee,[4,5] E. S. Choi,[4] Y. Y. Han,[1] L. S. Ling,[1] L. Pi,[1,2,7] Y. H. Zhang,[1,7] G. Chen,[6,7,*] Z. R. Yang,[1,7,8,†] H. D. Zhou,[9,10,‡] and X. F. Sun[2,7,8,§]

[1]*Anhui Province Key Laboratory of Condensed Matter Physics at Extreme Conditions, High Magnetic Field Laboratory, Chinese Academy of Sciences, Hefei, Anhui 230031, People's Republic of China*

[2]*Department of Physics, Hefei National Laboratory for Physical Sciences at Microscale, and Key Laboratory of Strongly-Coupled Quantum Matter Physics (CAS), University of Science and Technology of China, Hefei, Anhui 230026, People's Republic of China*

[3]*Fujian Institute of Research on the Structure of Matter, Chinese Academy of Sciences, Fuzhou, Fujian 350002, People's Republic of China*

[4]*National High Magnetic Field Laboratory, Florida State University, Tallahassee, Florida 32306-4005, USA*

[5]*Department of Physics, Florida State University, Tallahassee, Florida 32306-3016, USA*

[6]*State Key Laboratory of Surface Physics and Department of Physics, Center for Field Theory and Particle Physics, Fudan University, Shanghai, 200433, China*

[7]*Collaborative Innovation Center of Advanced Microstructures, Nanjing, Jiangsu 210093, People's Republic of China*

[8]*Institute of Physical Science and Information Technology, Anhui University, Hefei, Anhui 230601, People's Republic of China*

[9]*Key laboratory of Artificial Structures and Quantum Control (Ministry of Education), School of Physics and Astronomy, Shanghai JiaoTong University, Shanghai 200240, China*

[10]*Department of Physics and Astronomy, University of Tennessee, Knoxville, Tennessee 37996-1200, USA*

(Received 19 September 2017; revised manuscript received 8 March 2018; published 5 April 2018)

We report detailed dc and ac magnetic susceptibilities, specific heat, and thermal conductivity measurements on the frustrated magnet $ZnCr_2Se_4$. At low temperatures, with an increasing magnetic field, this spinel material goes through a series of spin state transitions from the helix spin state to the spiral spin state and then to the fully polarized state. Our results indicate a direct quantum phase transition from the spiral spin state to the fully polarized state. As the system approaches the quantum criticality, we find strong quantum fluctuations of the spins with behaviors such as an unconventional T^2-dependent specific heat and temperature-independent mean free path for the thermal transport. We complete the full phase diagram of $ZnCr_2Se_4$ under the external magnetic field and propose the possibility of frustrated quantum criticality with extended densities of critical modes to account for the unusual low-energy excitations in the vicinity of the criticality. Our results reveal that $ZnCr_2Se_4$ is a rare example of a 3D magnet exhibiting a field-driven quantum criticality with unconventional properties.

DOI: 10.1103/PhysRevLett.120.147204

Since the beginning of the century, quantum phase transition has emerged as an important subject in modern condensed matter physics [1]. Quantum phase transition and quantum criticality are associated with qualitative but continuous changes in relevant physical properties of the underlying quantum many-body system at an absolute zero temperature [1,2]. In the vicinity of quantum criticality, the low-energy and long-distance properties are controlled by the quantum fluctuation and the critical modes of the phase transition such that certain interesting and universal scaling laws could arise. It is well known that quantum criticality often occurs in the system with competing interactions where different interactions favor distinct phases or orders. Many physical systems such as high-temperature superconducting cuprates [2], heavy fermion and Kondo lattice materials [3], Fermi liquid metals with spin density wave instability [4], and Mott insulators have been proposed to be realizations of quantum criticality [1]. For superconductors and metals, the multiple low-energy degrees of freedom and orders may complicate the critical phenomena and the experimental interpretation. In contrast, Mott insulators with large charge gaps are primarily described by spin and/or orbital degrees of freedom and may have the advantage of simplicity in revealing critical behaviors.

The Ising magnets $CoNb_2O_6$ and $LiHoF_4$ in external magnetic fields realize the quantum Ising model and transition [5–10]. External magnetic fields in dimerized magnets like Han purple $BaCuSi_2O_6$ [11,12] induce a triplon Bose-Einstein condensation transition. In a more complicated example of the diamond lattice antiferromagnet $FeSc_2S_4$ [13–17], it is the competition between the superexchange interaction and the on-site spin-orbital coupling that drives a quantum phase transition from the antiferromagnetic order to the spin-orbital singlet phase [18,19]. These known examples of quantum phase transitions in strong Mott insulating materials with spin degrees of

freedom are described by simple Ising or Gaussian criticality where there are a discrete number of critical modes governing the low-energy properties. In this Letter, we explore the magnetic properties of a three-dimensional frustrated magnetic material $ZnCr_2Se_4$. From the thermodynamic, dynamic susceptibility, and thermal transport measurements, we demonstrate that there exists a field-driven quantum criticality with unusual properties such as a T^2-dependent specific heat and temperature-independent mean free path for thermal transport. Our quantum criticality has extended numbers of critical modes and is beyond the simple Ising or Gaussian criticality among the existing materials that have been reported before.

In the spinel compound $ZnCr_2Se_4$, the Cr^{3+} ion hosts the localized electrons and gives rise to the spin-3/2 (Cr^{3+}) local moments that form a 3D pyrochlore lattice. The reported dielectric polarization [20], magnetization and ultrasound [21], and neutron and synchrotron x-ray [22,23] studies have shown that, with an increasing magnetic field, this system goes from a helix spin state to a spiral spin state to an unidentified regime and then a fully polarized state at the measured temperatures. Two possibilities have been proposed for this unidentified regime: an umbrella state and a spin nematic state [21,24]. Both the umbrella state and a spin nematic state break the spin rotational symmetry. We address this unidentified regime by completing the magnetic phase diagram of $ZnCr_2Se_4$ with dc and ac susceptibility, specific heat, and thermal conductivity measurements. We do not observe signatures of symmetry breaking in the previously unidentified regime down to the lowest measured temperature. We attribute our experimental results to a quantum critical point (QCP) between the spiral spin state and the polarized state and identify the previously unidentified regime as the quantum critical regime.

The experimental details are listed in Supplemental Material [25]. The dc magnetization measured at 0.01 T in Fig. 1(a) shows a pronounced peak at $T_N = 21$ K, corresponding to the antiferromagnetic (AFM) order accompanied by a cubic to tetragonal structural transition as previously reported [22]. With increasing fields, the peak shifts to lower temperatures. The dc magnetization measured at 0.5 K in Fig. 1(b) shows an anomaly near $H_{C1} \sim 1.6$ T, which is more evident as a peak on the dM/dH curve. As previous studies reported, the magnetic domain reorientation occurs at this critical field H_{C1} and, above which, the helix spin structure is transformed into a tilted conical one [20–23]. Because of the reorientation of magnetic domains, the magnetization displays hysteresis when the field is ramping down below H_{C1}. This reorientation is also revealed as an irreversibility between the ZFC and FC curves below 8 K for the susceptibility measured at 0.01 T, while it is suppressed completely at $H \geq 1.7$ T.

The real part of ac susceptibility χ' in Fig. 2(a) clearly shows two peaks at H_{C1} and H_{C2}. Here, H_{C1} is consistent

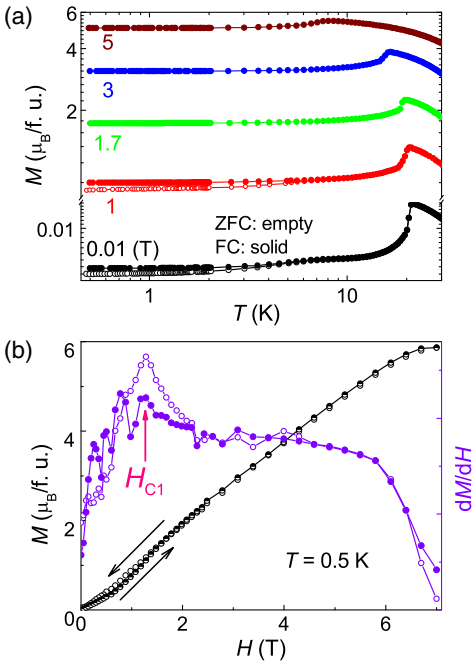

FIG. 1. (a) The temperature dependence of zero field cooling (ZFC) and field cooling (FC) dc magnetizations at different applied fields. (b) The dc magnetization measured at 0.5 K and its dM/dH curve.

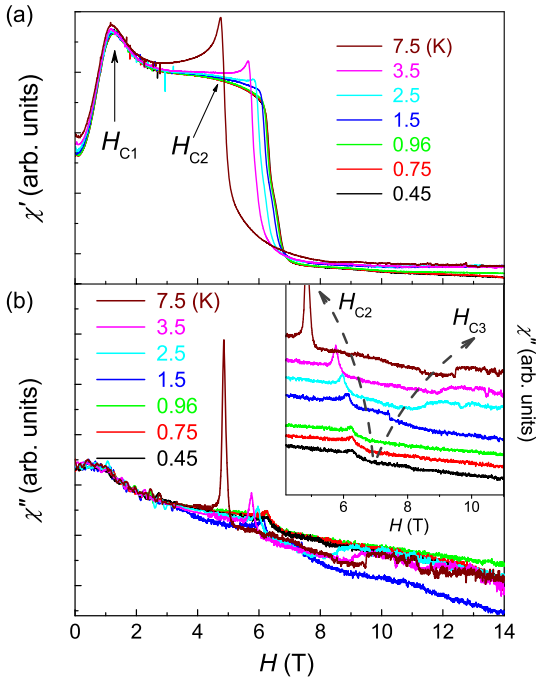

FIG. 2. The magnetic field dependence of ac susceptibility at several temperatures: (a) the real component; (b) the imaginary component. The inset in (b) shows the enlargement of the high-field data. The arrows indicate the evolution of high-field anomalies with increasing temperatures.

with the H_{C1} obtained from the magnetization data above. H_{C2} is consistent with the reported H_{C2} value, above which the spiral spin structure is suppressed with a concomitant structure transition from tetragonal to cubic. Meanwhile, a small bump at H_{C1}, a sharp peak at H_{C2}, and a steplike anomaly near 9.5 T are clearly seen for the imaginary part (χ'') measured at 7.5 K. This steplike anomaly is in accordance with the plateau observed from the sound velocity measurements around 10 T at 2 K, which has been correlated to the onset of a fully polarized magnetic phase at H_{C3} [21]. Upon further cooling, H_{C3} moves to lower fields and is hardly discernible below 1.5 K from the ac susceptibility measurement, while H_{C2} shifts to higher fields [see the inset in Fig. 2(b)].

At a zero magnetic field, the specific heat in Fig. 3(a) shows a sharp peak at $T_N = 21$ K, which shifts to a lower temperature with an increasing magnetic field and disappears completely at 6.5 T. Moreover, a small low-temperature hump around 1–2 K is observed at a zero magnetic field, which is enhanced with an increasing field up to 6.5 T and then strongly suppressed at 10 T. This kind of field dependence is very different from the usual Schottky anomaly of magnetic specific heat. Therefore, this anomaly could be originated from the spin fluctuations. It is consistent with the recent neutron-diffraction studies that reveal broad diffuse scattering due to spin fluctuations in the long-range-ordered state at temperatures down to 4 K [22,23]. The strongest hump at 6.5 T suggests stronger spin fluctuations around this field. Below 1 K, we tend to fit the heat capacity data at 6.5 T with a γT^{α} behavior. The obtained result is T^2 down to the lowest temperature of 0.06 K. Here we assume

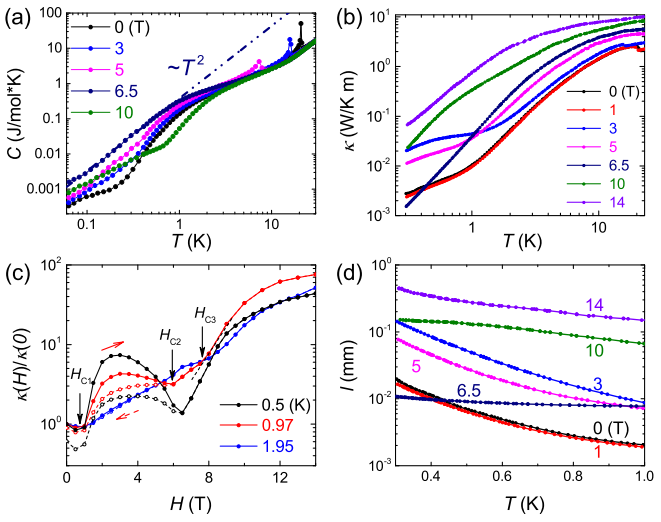

FIG. 3. (a) The temperature dependence of the specific heat at several magnetic fields from 0.06 to 30 K. The dashed line represents the T^2 dependence. (b) The temperature dependence of the thermal conductivity from 0.3 to 30 K at various magnetic fields. (c) The field dependence of the thermal conductivity at selected temperatures below 2 K. (d) The calculated mean free path.

that the lattice contribution of specific heat at such low temperatures is negligible, and then the T^2 behavior for 6.5 T data is abnormal for a 3D magnet.

To further manifest the dynamic properties of the system under the magnetic field, we carry out the thermal conductivity measurement. As we depict in Fig. 3(b), the thermal conductivity κ at 0 T shows a structural-transition-related anomaly at $T_N = 21$ K and a strong weakness of the $\kappa(T)$ slope around 1 K that should be related to the spin fluctuations observed from the specific heat. With an increasing magnetic field, T_N shifts to lower temperatures and disappears at $H \geq 5$ T. The slope change around 1 K is not sensitive to the magnetic field but diminishes at $H \geq 6.5$ T. While the κ mainly shows a gradual increase with an increasing magnetic field at high temperatures ($T > 3$ K), its field dependence is complicated at low temperatures ($T < 1$ K), which is more clearly demonstrated in Fig. 3(c).

At 1.95 K, the $\kappa(H)/\kappa(0)$ curve in Fig. 3(c) shows three weak anomalies at ~1, 5.5, and 8 T, which correspond to H_{C1}, H_{C2}, and H_{C3}, respectively. At H_{C1}, a spin reorientation appears, which is related to a minimizing of the anisotropy gap and a sudden increase of the AFM magnon excitations. This could cause an enhancement of magnon scattering on phonons and the low-field decrease of κ. The second anomaly at H_{C2}, which becomes clearer at 0.97 K, is demonstrated as a diplike suppression of κ and is likely due to the spin fluctuations at H_{C2}. The third anomaly at H_{C3}, identified as a quicker increase of κ, is apparently due to the strong suppression of spin fluctuations associated with the transition or crossover from that unidentified regime to the fully polarized spin state. The spin fluctuations are strongly suppressed in the fully polarized spin state, because the spin excitation is gapped at low energies. At lower temperatures that were not accessed in the previous experiments [20–23], the anomalies at H_{C2} and H_{C3} tend to merge, consistent with the opposite temperature dependencies of these two critical fields observed from our ac susceptibility measurement. In particular, at 0.5 K these two anomalies merge into a single one at 6.5 T, and the $\kappa(H)/\kappa(0)$ curve shows a deep valley at the background of field-induced enhancement. This is consistent with the specific heat result showing that the spin fluctuation is the strongest around 6.5 T. As we will explain in detail, both the specific heat and the thermal transport results suggest the existence of the quantum criticality at 6.5 T.

Before getting onto our interpretation, we here calculate the phonon mean free path from κ using a standard method [30]. We choose the Debye temperature to be 308 K [31] and assume κ is primarily phononic. The results are depicted in Fig. 3(d). At 0 T, the phonon mean free path ($l \sim 10^{-2}$ mm) is nearly 2 orders of magnitude smaller than the sample size (~1 mm) even at the lowest temperature of 0.3 K. This means that the phonon scattering is still active at such low temperatures. Since the phonon scatterings caused by phonons, impurities, and other crystal defects are

known to be quenched at low temperatures, there must be some magnetic scattering processes. Also, because of the small mean free path l, the magnetic excitations are not likely to make a sizable contribution to the heat transport. With increasing magnetic fields, l is generally enhanced, indicating a suppression of magnetic scatterings. Under the highest field of 14 T, the phonon mean free path approaches the sample size, which indicates the complete suppression of spin fluctuations in the polarized state. This is consistent with the gapped spin excitations for the fully polarized spin state. In contrast, at 6.5 T, l drops back to 10^{-2} mm size with no obvious temperature dependence below 1 K.

A detailed H-T phase diagram of $ZnCr_2Se_4$ was constructed in Fig. 4 by using the phase transition temperatures and critical fields obtained from our above measurements. By comparing to the reported phase diagram [21], two important new features were observed in this full phase diagram with lower temperatures and higher magnetic fields. One is that the phase transition temperature for the spiral spin structure is suppressed to a zero temperature with increasing fields before the system enters the fully polarized state. Therefore, there is a direct quantum phase transition between the spiral spin state and the polarized phase, and this transition is marked as the QCP in Fig. 4. The other one is that the previous unidentified regime between the spiral state and the fully polarized state does not persist down to the lowest temperature. Note that our measurements were carried out at a much lower temperature than the previous reports. Thus, in Fig. 4, this previously unidentified regime is naturally identified as the quantum critical regime that is the finite temperature extension of the quantum criticality.

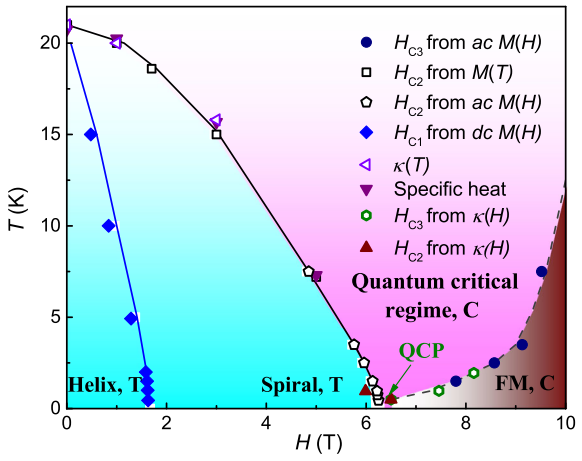

FIG. 4. The H-T phase diagram of $ZnCr_2Se_4$. "T" and "C" refer to the tetragonal and the cubic structure, respectively. "Helix," "Spiral," and "FM" stand for the helix spin state, spiral spin state, and spin-fully polarized state, respectively. A QCP is deduced between the spiral spin state and the polarized phase. The solid (dashed) boundary refers to an actual phase transition (crossover). The pink region is marked as the quantum critical regime. See the main text for a detailed discussion.

Why is the previously unidentified regime not an umbrella state or a spin nematic state? As we have pointed out earlier, both states break the spin rotational symmetry, and the former may break the lattice translation. This is a 3D system, and this kind of symmetry breaking should persist down to a zero temperature and cover a finite parameter regime. This finite-range phase is not observed at the lowest temperature. For the same reason, the symmetry should be restored at high enough temperatures via a phase transition. Such a thermodynamic phase transition is clearly not observed in the heat capacity and thermal transport measurements.

The spin spiral state and the fully polarized state are distinct phases with different symmetry properties. The latter is translational invariant and fully gapped, while the former breaks the lattice symmetry and spin rotational symmetry. There must be a phase transition separating them, and this quantum phase transition is manifested as the QCP at 6.5 T in Fig. 4. What is the property of this criticality? The heat capacity was found to behave as T^2 at low temperatures at the QCP, indicating a much larger density of states than the simple Gaussian fixed point. For a Gaussian fixed point, we would expect the heat capacity as T^3 up to a logarithmic correction due to the critical fluctuations. The T^2 heat capacity suggests that the low-energy density of states should scale as $D(\epsilon) \sim \epsilon$ with the energy ϵ. We know that the nodal line semimetal with symmetry and topologically protected line degeneracies has this extended density of states when the Fermi energy is tuned to the degenerate point [32]. However, our system is purely bosonic with spin degrees of freedom, and there is no emergent fermionic statistics. To support $D(\epsilon) \sim \epsilon$ at the QCP, we would have the critical modes be degenerate or almost degenerate along the lines in the reciprocal space such that the current thermodynamic measurement cannot resolve them. It has been known that the frustrated spin interactions could lead to such line degeneracies for the critical modes and the resulting frustrated quantum criticality [33,34]. The possibility that infinite modes with line degeneracies become critical at the same time is an unconventional feature of this QCP. These critical modes scatter the phonon strongly and suppress the thermal transport near the criticality. It will be interesting to directly probe these degenerate modes with inelastic neutron scattering and explore the fates of the critical modes on both sides of the QCP. Our thermal transport results also call for further theoretical effects on the scattering between the extended density of critical modes and the low-energy phonons near the criticality.

Finally, the system displays different lattice structures for different magnetic phases in the phase diagram. Both the helix and the spiral spin states have tetragonal structure, while the quantum critical regime and the fully polarized state have cubic structure. This is simply the consequence of the spin-lattice coupling. The helix and the spiral spin states break the lattice cubic symmetry, and this symmetry is transmitted to the lattice via the spin-lattice coupling. The quantum critical regime and the fully polarized state are

uniform states and restore the lattice symmetry. The correlation between the sound velocity and the magnetic structure in the previous experiments has a similar origin [21].

In summary, by completing the H-T phase diagram of $ZnCr_2Se_4$, we demonstrate the existence of the QCP and quantum critical regime induced by an applied magnetic phase in this 3D magnet. Our finding of the unconventional quantum criticality calls for future works and is likely to provide a unique example of frustrated quantum criticality for further studies.

This research was supported by the National Key Research and Development Program of China (Grant No. 2016YFA0401804), the National Natural Science Foundation of China (Grants No. 11574323 and No. U1632275), and the Natural Science Foundation of Anhui Province (Grant No. 1708085QA19). X. F. S. acknowledges support from the National Natural Science Foundation of China (Grants No. 11374277 and No. U1532147), the National Basic Research Program of China (Grants No. 2015CB921201 and No. 2016YFA0300103), and the Innovative Program of Development Foundation of Hefei Center for Physical Science and Technology. G. C. thanks the support from the Ministry of Science and Technology of China with Grant No. 2016YFA0301001, the initiative research funds and the program of first-class University construction of Fudan University, and the Thousand-Youth-Talent Program of China. H. D. Z. thanks the support from the Ministry of Science and Technology of China with Grant No. 2016YFA0300500 and from NSF-DMR with Grant No. NSF-DMR-1350002. Z. Y. Z. acknowledges support from the National Natural Science Foundation of China (Grant No. 51702320). M. L. and E. S. C. acknowledge support from NSF-DMR-1309146. The work at NHMFL is supported by NSF-DMR-1157490 and the State of Florida. The x-ray work was performed at HPCAT (Sector 16), Advanced Photon Source, Argonne National Laboratory. HPCAT operations are supported by DOE-NNSA under Award No. DE-NA0001974 and DOE-BES under Award No. DE-FG02-99ER45775, with partial instrumentation funding by NSF. The Advanced Photon Source is a U.S. Department of Energy (DOE) Office of Science User Facility operated for the DOE Office of Science by Argonne National Laboratory under Contract No. DE-AC02-06CH11357.

C. C. G. and Z. Y. Z. contributed equally to this work.

*gangchen.physics@gmail.com
†zryang@issp.ac.cn
‡hzhou10@utk.edu
§xfsun@ustc.edu.cn

[1] S. Sachdev, *Quantum Phase Transitions*, 2nd ed. (Cambridge University Press, Cambridge, England, 2011).
[2] S. Sachdev, Rev. Mod. Phys. **75**, 913 (2003).
[3] Q. Si and F. Steglich, Science **329**, 1161 (2010).
[4] H. v. Löhneysen, A. Rosch, M. Vojta, and P. Wölfle, Rev. Mod. Phys. **79**, 1015 (2007).
[5] R. Coldea, D. A. Tennant, E. M. Wheeler, E. Wawrzynska, D. Prabhakaran, M. Telling, K. Habicht, P. Smeibidl, and K. Kiefer, Science **327**, 177 (2010).
[6] T. Liang, S. M. Koohpayeh, J. W. Krizan, T. M. McQueen, R. J. Cava, and N. P. Ong, Nat. Commun. **6**, 7611 (2015).
[7] A. W. Kinross, M. Fu, T. J. Munsie, H. A. Dabkowska, G. M. Luke, Subir Sachdev, and T. Imai, Phys. Rev. X **4**, 031008 (2014).
[8] C. M. Morris, R. Valdés Aguilar, A. Ghosh, S. M. Koohpayeh, J. Krizan, R. J. Cava, O. Tchernyshyov, T. M. McQueen, and N. P. Armitage, Phys. Rev. Lett. **112**, 137403 (2014).
[9] H. M. Rønnow, J. Jensen, R. Parthasarathy, G. Aeppli, T. F. Rosenbaum, D. F. McMorrow, and C. Kraemer, Phys. Rev. B **75**, 054426 (2007).
[10] P. B. Chakraborty, P. Henelius, H. Kjønsberg, A. W. Sandvik, and S. M. Girvin, Phys. Rev. B **70**, 144411 (2004).
[11] M. Jaime, V. F. Correa, N. Harrison, C. D. Batista, N. Kawashima, Y. Kazuma, G. A. Jorge, R. Stein, I. Heinmaa, S. A. Zvyagin, Y. Sasago, and K. Uchinokura, Phys. Rev. Lett. **93**, 087203 (2004).
[12] T. Giamarchi, C. Rüegg, and O. Tchernyshyov, Nat. Phys. **4**, 198 (2008).
[13] V. Fritsch, J. Hemberger, N. Büttgen, E. W. Scheidt, H. A. Krug von Nidda, A. Loidl, and V. Tsurkan, Phys. Rev. Lett. **92**, 116401 (2004).
[14] A. Krimmel, M. Mücksch, V. Tsurkan, M. M. Koza, H. Mutka, and A. Loidl, Phys. Rev. Lett. **94**, 237402 (2005).
[15] N. J. Laurita, J. Deisenhofer, L. Pan, C. M. Morris, M. Schmidt, M. Johnsson, V. Tsurkan, A. Loidl, and N. P. Armitage, Phys. Rev. Lett. **114**, 207201 (2015).
[16] L. Mittelstädt, M. Schmidt, Z. Wang, F. Mayr, V. Tsurkan, P. Lunkenheimer, D. Ish, L. Balents, J. Deisenhofer, and A. Loidl, Phys. Rev. B **91**, 125112 (2015).
[17] A. Biffin, Ch. Rüegg, J. Embs, T. Guidi, D. Cheptiakov, A. Loidl, V. Tsurkan, and R. Coldea, Phys. Rev. Lett. **118**, 067205 (2017).
[18] G. Chen, L. Balents, and A. P. Schnyder, Phys. Rev. Lett. **102**, 096406 (2009).
[19] G. Chen, A. P. Schnyder, and L. Balents, Phys. Rev. B **80**, 224409 (2009).
[20] H. Murakawa, Y. Onose, K. Ohgushi, S. Ishiwata, and Y. Tokura, J. Phys. Soc. Jpn. **77**, 043709 (2008).
[21] V. Felea, S. Yasin, A. Gunther, J. Deisenhofer, H. A. K. von Nidda, S. Zherlitsyn, V. Tsurkan, P. Lemmens, J. Wosnitza, and A. Loidl, Phys. Rev. B **86**, 104420 (2012).
[22] F. Yokaichiya, A. Krimmel, V. Tsurkan, I. Margiolaki, P. Thompson, H. N. Bordallo, A. Buchsteiner, and N. Stüßer, D. N. Argyriou, and A. Loidl, Phys. Rev. B **79**, 064423 (2009).
[23] J. Akimitsu, K. Siratori, G. Shirane, M. Iizumi, and T. Watanabe, J. Phys. Soc. Jpn. **44**, 172 (1978).
[24] A. Miyata, H. Ueda, Y. Ueda, Y. Motome, N. Shannon, K. Penc, and S. Takeyama, J. Phys. Soc. Jpn. **81**, 114701 (2012).
[25] See Supplemental Material at http://link.aps.org/supplemental/10.1103/PhysRevLett.120.147204 for experimental details, which includes Ref. [26–29].

[26] C. C. Gu, Z. R. Yang, X. L. Chen, L. Pi, and Y. H. Zhang, J. Phys. Condens. Matter **28**, 18LT01 (2016).
[27] P. Zajdel, W. Y. Li, W. van Beek, A. Lappas, A. Ziolkowska, S. Jaskiewicz, C. Stock, and M. A. Green, Phys. Rev. B **95**, 134401 (2017).
[28] Z. L. Dun, M. Lee, E. S. Choi, A. M. Hallas, C. R. Wiebe, J. S. Gardner, E. Arrighi, R. S. Freitas, A. M. Arevalo-Lopez, J. P. Attfield, H. D. Zhou, and J. G. Cheng, Phys. Rev. B **89**, 064401 (2014).
[29] X. F. Sun, W. Tao, X. M. Wang, and C. Fan, Phys. Rev. Lett. **102**, 167202 (2009).
[30] Z. Y. Zhao, X. M. Wang, C. Fan, W. Tao, X. G. Liu, W. P. Ke, F. B. Zhang, X. Zhao, and X. F. Sun, Phys. Rev. B **83**, 014414 (2011).
[31] T. Rudolf, C. Kant, F. Mayr, J. Hemberger, V. Tsurkan, and A. Loidl, Phys. Rev. B **75**, 052410 (2007).
[32] A. A. Burkov, M. D. Hook, and L. Balents, Phys. Rev. B **84**, 235126 (2011).
[33] A. Mulder, R. Ganesh, L. Capriotti, and A. Paramekanti, Phys. Rev. B **81**, 214419 (2010).
[34] G. Chen, M. Hermele, and L. Radzihovsky, Phys. Rev. Lett. **109**, 016402 (2012).